Article

Not peer-reviewed version

Biomechanical Evaluation of a Biomimetic Stand-Assist Toilet Seat in Older Adults: A Synchronized AI-Kinematic and Kinetic Analysis

Shan-Ju Yeh , Shu-Yu Yang , Li-Chi Chao , Tsai-Sui Lu , Yu-Sheng Yang *

Posted Date: 10 April 2026

doi: 10.20944/preprints202604.0744.v1

Keywords: biomimetic trajectory; geriatrics; pose estimation

Preprints.org (www.preprints.org) | NOT PEER-REVIEWED | Posted: 10 April 2026 doi:10.20944/preprints202604.0744.v1

Article

Biomechanical Evaluation of a Biomimetic Stand-Assist Toilet Seat in Older Adults: A Synchronized AI-Kinematic and Kinetic Analysis

Shan-Ju Yeh [1], Shu-Yu Yang [2,3], Li-Chi Chao [4], Tsai-Sui Lu [1] and Yu-Sheng Yang [1,5,*]

1 Department of Physical Medicine and Rehabilitation, Kaohsiung Medical University Chung-Ho Memorial Hospital, Kaohsiung, Taiwan
2 Department of Physical Medicine and Rehabilitation, Chi Mei Medical Center, Tainan City, Taiwan
3 Department of Occupational Therapy, Shu-Zen Junior College of Medicine and Management, Kaohsiung, Taiwan
4 Division of Health Promotion, Footwear & Recreation Technology Research Institute, Taichung, Taiwan
5 Department of Occupational Therapy, Kaohsiung Medical University, Kaohsiung, Taiwan
* Correspondence: yusheng@kmu.edu.tw

Abstract

Modern residential toilets pose a significant biomechanical challenge for older adults with diminished muscle strength, as standard seat heights necessitate excessive joint range of motion (ROM) and compensatory upper-limb reliance. This study evaluated the biomechanical efficacy of a biomimetic Stand-assist Toilet Seat designed to facilitate sit-to-stand (STS) transitions through a proactive curvilinear trajectory. Thirty community-dwelling older adults were stratified into high-, moderate-, and low-functioning groups based on 30-second Chair Stand Test normative data. A multi-modal assessment framework was employed, integrating MediaPipe-based AI pose estimation for joint kinematics and instrumented armrests with high-precision load cells for kinetic analysis. The results demonstrated that the biomimetic seat significantly optimized movement efficiency, evidenced by a robust reduction in hip and knee ROM with a large effect size ($\eta^2_p > .70$, $p<.001$). Kinetic data further revealed substantial upper-limb unloading, with significant decreases in peak arm-support force (*Fmax*, p=.001, η^2_p =.35) and cumulative impulse (I_{arm}, $p<.001$, η^2_p =.42). While no significant interaction was found, a clinical trend (η^2_p =.17) suggested that low-functioning individuals derived the greatest mechanical advantage from the device. By actively guiding the user's center of mass toward a biomechanically advantageous "power zone," the biomimetic trajectory minimizes compensatory trunk flexion and armrest reliance. These findings provide evidence-based insights into the role of trajectory-informed assistive technology in enhancing toileting safety and functional independence for the aging population, particularly those exhibiting signs of possible sarcopenia.

Keywords: biomimetic trajectory; geriatrics; pose estimation

---

1. Introduction

The global demographic shift toward an aging population has intensified the emphasis on maintaining functional independence among older adults. Among the essential Activities of Daily Living (ADLs), the sit-to-stand (STS) transition is a mechanically demanding task, requiring substantial lower-limb joint torque and coordinated whole-body movement [1–3]. Impairments in STS performance are strongly associated with reduced mobility [4,5], increased fall risk [6,7], and loss of independence [8,9].

Biomechanically, the STS movement is divided into four phases: flexion-momentum, momentum-transfer, extension, and stabilization [10]. The initial flexion-momentum phase is critical;

it involves forward trunk inclination to generate horizontal momentum prior to seat-off [1,11,12]. Insufficient trunk flexion often results in inadequate anterior center-of-mass (COM) transfer, forcing older adults to seek external stabilization. In toileting contexts, where standard seats are typically low, the increased hip and knee joint ROM and extensor moments often exceed the physiological capacity of sarcopenic older adults, leading to a heavy reliance on upper-limb compensatory strategies—specifically, pushing on armrests to supplement the required vertical thrust.

To mitigate these challenges, the BSTS evaluated in this study incorporates a biomimetic forward-tilting motion that replicates natural kinematic synergy. This pre-positioning facilitates efficient anterior COM displacement, potentially shifting the mechanical workload from the user's internal joint moments to the device's external assistance. However, a critical research gap remains: while kinematic improvements are often documented, the synchronous reduction in compensatory upper-limb loading remains under-explored. Excessive reliance on armrests not only indicates lower-limb insufficiency but also increases the risk of shoulder strain and falls if the grip slips.

In this study, we propose a multi-modal assessment framework that extends beyond sagittal-plane kinematics. In addition to quantifying hip and knee joint ROM using a MediaPipe-based pose estimation approach, we integrated a high-precision force sensor into the instrumented armrests. This allows for the simultaneous quantification of upper-limb support forces during the transition. We hypothesize that the biomimetic trajectory of the Stand-assist Toilet Seat will optimize the user's mechanical advantage, thereby reducing the peak force required on the armrests compared to conventional toilet seats. By integrating AI-driven kinematic analysis with synchronized kinetic sensing, this research seeks to provide a comprehensive evidence-based insight into how trajectory-informed assistive technologies can minimize physical strain and enhance toileting safety for the elderly.

2. Materials and Methods

2.1. Participants

A total of 30 community-dwelling older adults aged 65 years and above were recruited. Inclusion criteria were: (1) age ≥ 65 years; (2) ability to perform the sit-to-stand (STS) task (with upper-limb assistance if necessary); and (3) cognitive ability to follow multi-step verbal instructions. Participants were excluded if they presented with acute musculoskeletal injuries, severe neurological disorders (e.g., Parkinson's disease, stroke), or symptomatic orthostatic hypotension that would compromise safety during repeated STS trials.

All participants provided written informed consent prior to participation. The study was conducted in accordance with the Declaration of Helsinki and adhered to Good Clinical Practice guidelines and was approved by the Institutional Review Board of Kaohsiung Medical University Chung-Ho Memorial Hospital (KMUHIRBE(II)20250259).

Participants were stratified into three functional tiers (n=10 per group) based on the 30-second Chair Stand Test (CST) normative data:

High-functioning group ($P \geq 70$): Participants who performed at or above the 70th percentile, representing above-average lower-limb functional strength.

Moderate-functioning group ($30 \leq P < 70$): Participants who performed between the 30th and 70th percentiles, representing average functional performance.

Low-functioning group ($P < 30$): Participants scoring below the 30th percentile or unable to complete the 30s-CST without armrest support. This group exhibited "possible sarcopenia" and a clinical reliance on upper-limb compensatory strategies, highlighting their functional need for assistive technology.

2.2. Apparatus and Experimental Setup

The experimental environment was configured to simulate a domestic restroom setting. Two distinct seating conditions were evaluated：(1) Conventional toilet (control condition): A standard

 doi:10.20944/preprints202604.0744.v1

pedestal toilet (seat height: 40 cm) equipped with bilateral fixed armrests; (2) Biomimetic Stand-assist Toilet Seat (BSTS, experimental condition): A power-assisted device designed to provide a dynamic, curvilinear lifting trajectory. This device was also equipped with bilateral armrests, with dimensions matched to those of the control condition (Figure 1).

To quantify upper-limb reliance, both systems were equipped with instrumented armrests featuring high-precision load cells mounted beneath the armrests. These sensors recorded the vertical reaction forces exerted by participants' upper limbs. Kinetic data were sampled at 100 Hz. The kinematic data were captured at 60 frames per second (fps) using a high-definition red-green-blue (RGB) camera (PW513, AVerMedia, Taiwan) positioned 2.5 meters from the participant in the sagittal plane. This setup enabled synchronized collection of video data for AI-based pose estimation using MediaPipe, along with kinetic data from the instrumented armrests (Figure 1).

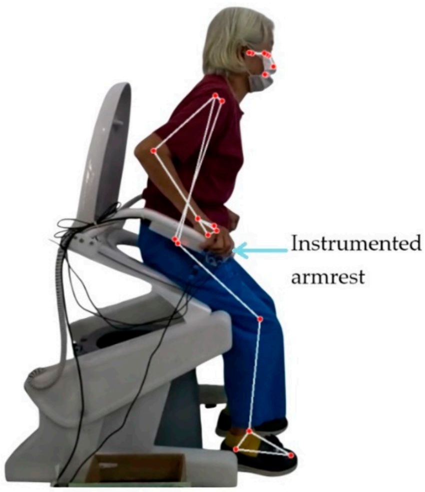

Figure 1. BSTS with instrumented armrests; pose detection via MediaPipe.

2.3. Experimental Procedure

All participants completed the experimental protocol in a single session. Upon arrival, participants' demographic data, including age, sex, height, and body weight, were recorded. Following familiarization trials, participants performed three STS trials under two conditions: (1) conventional toilet and (2) BSTS. The order of the conditions was randomized to minimize potential order effects. To replicate ecological validity, participants were instructed to "stand up at a comfortable pace" and were explicitly permitted to use the armrests as needed. This allowed for the assessment of natural compensatory behavior. A 1-minute seated rest was enforced between trials to prevent muscle fatigue.

2.4. Data Processing

The recorded video data were processed using the MediaPipe Pose framework [13,14]. This approach extracted 33 skeletal landmarks per frame in two-dimensional coordinates (x, y). To improve data quality, a second-order Butterworth low-pass filter with a cut-off frequency of 6 Hz was applied to the raw coordinate data to attenuate high-frequency noise associated with computer vision-based tracking. The analysis focused on key sagittal plane landmarks to compute joint angles:

Hip joint angle: Defined by the angle formed between the acromion (shoulder), greater trochanter (hip), and lateral epicondyle (knee).

Knee joint angle: Defined by the angle formed between the greater trochanter (hip), lateral epicondyle (knee), and lateral malleolus (ankle).

Peak arm-support force (F_{max}) was defined as the maximum downward force (N) exerted on the armrests during the STS transition. This value was normalized to each participant's body weight and expressed as a percentage (%BW) to facilitate inter-participant comparisons. The impulse of arm

 doi:10.20944/preprints202604.0744.v1

support (I_{arm}, %BW•s) was defined as the time integral of the normalized arm-support force during the STS transition, representing the cumulative mechanical contribution of the upper limbs.

$$I_{arm} = \int_{t_{start}}^{t_{stop}} F(t)dt$$

where t_{start}(movement onset) was defined as the instant when the vertical displacement of the acromion process (shoulder landmark) exceeded three standard deviations, and t_{end} (stability) was reached when the vertical knee extension velocity returned to zero. Kinetic data were downsampled to 60 Hz to ensure temporal synchronization with the kinematic video frames.

2.5. Statistical Analysis

Descriptive statistics (mean ± standard deviation) were calculated for all outcome variables, including peak arm-support force (F_{max}), arm-support impulse (I_{arm}), and hip/knee joint angles. A 2×3 mixed-design analysis of variance (ANOVA) was employed to evaluate the main effects of seating condition (within-subject factor: control vs. experimental) and functional group (between-subject: High vs. Moderate vs. Low), as well as their interaction. Normality and homoscedasticity were verified via Shapiro-Wilk and Levene's tests, respectively. When significant main effects or interaction effects were identified, post hoc comparisons with Bonferroni correction were performed. Effect sizes were reported using partial eta squared (η^2_p) for ANOVA analyses to quantify the magnitude of observed effects. All statistical analyses were performed using appropriate statistical software (SPSS, version 20; IBM Corp., Armonk, NY, USA). The level of statistical significance was set at $\alpha = 0.05$.

3. Results

3.1. Participant Characteristics

Thirty community-dwelling older adults successfully completed the experimental protocol without any adverse events. Participants were stratified into three functional groups (n = 10 per group). There were no significant differences in age, height, or body weight among the three groups ($p > 0.05$), ensuring that the groups were well-matched in terms of basic physical characteristics (Table 1).

Table 1. Participant Characteristics.

Demographic characteristics	High (n=10)	Moderate (n=10)	Low (n=10)	p-value
Age (years, SD)	74.20(5.59)	69.90(7.01)	69.80(4.54)	0.17
Height (cm, SD)	152.89(4.11)	159.95(10.63)	156.02(8.46)	0.17
Weight (kg, SD)	53.79(5.91)	60.75(17.45)	67.35(11.41)	0.07

Note: SD = Standard Deviation.

3.2. Peak Arm-Support Force (F_{max})

A two-way mixed ANOVA revealed a significant main effect of seating condition (F (1,27) = 14.57, p = .001, η^2_p = .35), indicating that the measured outcome differed significantly between the conventional and biomimetic conditions (Table 2). A significant main effect of functional group was also observed (F (2,27) = 4.29, p = .024, η^2_p = .24), suggesting that performance differed across functional

 doi:10.20944/preprints202604.0744.v1

levels. However, the interaction effect between seating condition and functional group was not statistically significant (F (2,27) = 1.21, p = .31, η^2_p = .08), indicating that the effect of the BSTS was consistent across all groups.

Table 2. Comparison of peak arm-support force and cumulative impulse between conventional and biomimetic seating conditions across functional groups.

Kinetic Parameters		Biomimetic Mean (SD)	Control Mean (SD)	*p*-value: Between-group effect	*p*-value: Intragroup effect	*p*-value: Interaction effect
F_{max} (%BW)						
	High	17.03 (7.40)	21.15 (10.10)	0.001**	0.024**	0.314
	Moderate	21.87 (13.98)	26.94 (15.69)			
	Low	7.40 (4.58)	17.50 (3.33)			
I_{arm} (%BW•S)						
	High	17.11 (12.46)	28.96 (12.16)	<0.001**	0.089	0.214
	Moderate	26.51 (28.01)	40.92 (21.14)			
	Low	6.77 (5.32)	35.32 (15.24)			

Note: ** indicates statistical significance p<0.01; SD = Standard Deviation. *Fmax* is normalized to body weight (%BW); I_{arm} is calculated as the time integral of normalized force (%BW·s). Values are presented as Mean (SD).

3.3. Arm-Support Impulse (I_{arm})

For arm-support impulse, a significant main effect of seating condition was found for arm-support impulse (F (1,27) = 5.78, p <.001, η^2_p = .42), demonstrating that the biomimetic device substantially reduced the cumulative upper-limb loading during the STS transition (Table 2). Moreover, the main effect of functional group approached statistical significance (F (2,27) = 2.64, p = .089, η^2_p = .16), suggesting a trend toward differences in arm-support impulse across functional levels. Although the interaction effect between condition and functional group did not reach statistical significance (F (2,27) = 1.63, p = .21, η^2_p = .11), a moderate effect size was observed, indicating a potential trend toward differential effects across functional levels.

3.4. Hip Joint Angle

Analysis of hip joint kinematics revealed a robust main effect of the seating condition (Figure 2). Specifically, hip joint ROM was significantly altered between the two conditions (F (1,27) = 133.56, p < .001, η^2_p = .83), reflecting a substantial shift in movement amplitude. In contrast, neither the functional group (F (2,27) = 2.18, p = .13, η^2_p = .14) nor the interaction between seating condition and group (F (2,27) = 0.23, p = .79, η^2_p = .02). reached statistical significance. These findings imply that the biomimetic seat trajectory exerts a consistent influence on hip ROM across all functional levels.

Furthermore, the minimum hip joint angle was notably impacted by the seat condition (F (1,27) = 124.07, p < .001, η^2_p = .82). As illustrated in Figure 2, the biomimetic condition led to a larger minimum angle, indicating a significant reduction in peak hip flexion compared to the conventional setup. This kinematic adaptation remained uniform regardless of the participants' functional status, as evidenced by non-significant effects for both group (F (2,27) = 2.59, p = .16 η^2_p = .16) and interaction (F (2,27) = 0.84, p = .44, η^2_p = .06).

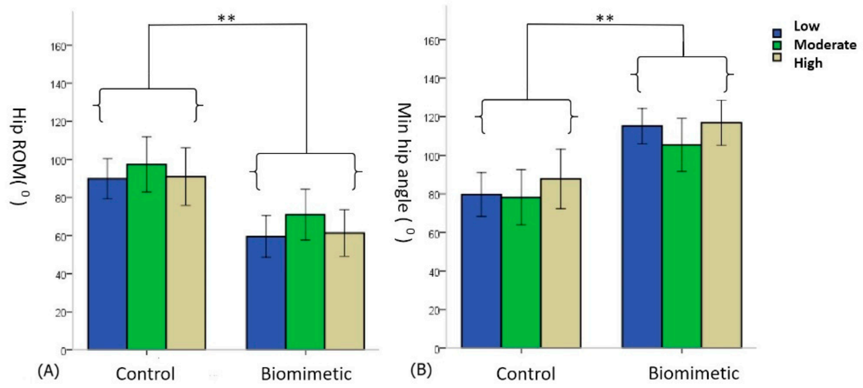

Figure 2. Comparison of hip kinematics between control and biomimetic seating conditions. (A) Hip ROM; (B) Minimum hip flexion angle. Data are presented as mean ± SD. Double asterisks (**) indicate *p* value <0.001.

3.5. Knee Joint Angle

Regarding knee joint kinematics, the seating condition emerged as the primary determinant of movement patterns (Figure 3). Knee ROM exhibited marked differences between conditions (F (1,27) = 73.85, p < .001, η^2_p = .73), whereas the functional group (F (2,27) = 2.99, p = .07, η^2_p = .18) and the condition-by-group interaction (F (2,27) = 1.62, p = .22, η^2_p = .11) showed no significant influence. These results suggest that the biomimetic trajectory modifies knee excursion in a manner independent of the user's physical capacity.

As illustrated in Figure 3, a similar pattern manifested in the minimum knee joint angle, which was significantly influenced by the seating condition (F (1,27) = 83.32, p < .001, η^2_p = .76). Under the biomimetic condition, participants demonstrated a reduction in peak knee flexion (represented by an increased minimum angle) relative to the control condition. This effect was stable across functional status, with no significant findings for group (F (2,27) = 1.73, p = .19, η^2_p = .11) or interaction (F (2,27) = 1.54, p = .23, η^2_p = .10), further confirming the universal kinematic shift induced by the experimental seat.

The maximum hip/knee joint angle, which occurred near full extension at the end of the STS movement, showed minimal variability across conditions and was therefore not considered a sensitive indicator for statistical comparison.

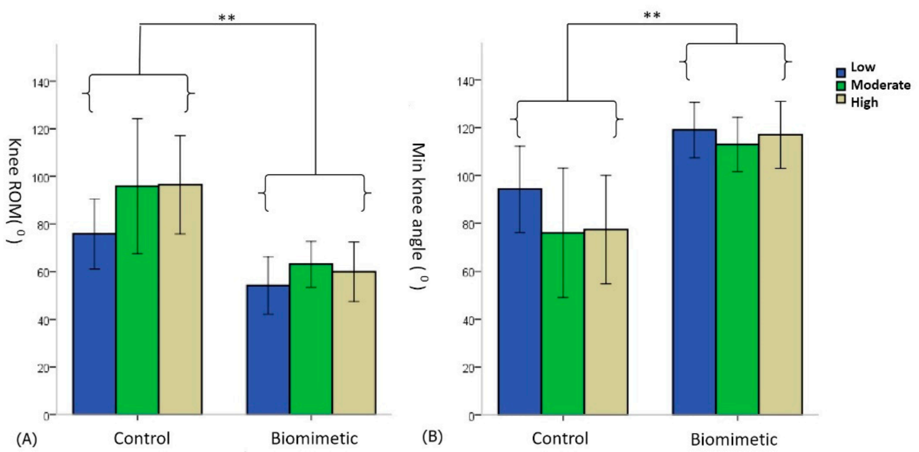

Figure 3. Comparison of knee kinematics between control and biomimetic seating conditions. (A) Knee ROM; (B) Minimum knee flexion angle. Data are presented as mean ± SD. Double asterisks (**) indicate *p* value <0.01.

4. Discussion

The primary objective of this study was to quantify the biomechanical advantages of a BSTS compared to a conventional seat among older adults with varying functional capacities. Our findings demonstrate that the curvilinear lifting trajectory significantly optimizes both the kinematics of the lower limbs and the kinetics of upper-limb reliance during the sit-to-stand (STS) transition.

4.1. Kinetic Implications: Reducing Upper-Limb Compensatory Reliance

The significant reduction in F_{max} and I_{arm} across all groups (p <.01) suggests that the biomimetic device effectively alleviates the mechanical burden on the upper extremities. In conventional low-seated toileting, sarcopenic older adults often reach their physiological limit for knee extensor torque, forcing a heavy reliance on the armrests to "pull" or "push" the body upward [15]. Our findings demonstrate that the biomimetic trajectory provides a crucial mechanical advantage that mitigates this compensatory demand.

Interestingly, the main effect of the functional group for I_{arm} approached statistical significance (p =0.089), suggesting a trend where baseline functional capacity naturally dictates the degree of arm-support reliance. More importantly, while the interaction effect did not reach statistical significance (p =0.21), the descriptive data reveals a transformative effect specifically for the Low-functioning group. In the conventional condition, these individuals exhibited the highest reliance on arm-support impulse (35.32 %BW•s), likely due to insufficient knee extensor torque to generate the necessary vertical momentum. However, under the biomimetic condition, their impulse dropped dramatically to 6.77 %BW•s—a level even lower than that of the High-functioning group under s conventional conditions. This highlights that the biomimetic trajectory provides the most "precise assistance" to those who lack the physiological reserves to stand independently. By providing this external "power boost," the device minimizes the risk of shoulder impingement and wrist strain, which are common secondary injuries in elderly populations who over-rely on manual supports for daily mobility [16].

4.2. Kinematic Optimization

The most striking kinematic finding was the massive effect size observed in hip and knee excursions (η^2_p >.70)., indicating a fundamental reorganization of the STS strategy. This optimization stems from the device's ability to facilitate an early anterior displacement of the COM. In conventional STS, older adults—particularly those in the low-functioning group—must perform exaggerated trunk flexion to shift their COM forward over the base of support before lift-off [10,11,17]. This compensatory "rocking" or "leaning" strategy is often a necessary response to diminished knee extensor strength, as it utilizes trunk momentum to assist in rising [18–20]. However, such extreme flexion is mechanically inefficient and significantly increases the risk of posterior balance loss or "seat-back" falls if the momentum is not perfectly controlled.

By contrast, the biomimetic seat's synchronized upward and forward lifting motion actively guides the user's COM toward the target standing position. This proactive mechanical assistance maintains the user within a biomechanically advantageous "power zone"—characterized by optimal muscle length-tension relationships and reduced gravitational moment arms—throughout the transition phase. Consequently, participants are relieved from the necessity of excessive trunk flexion, sustaining a more upright and stable posture.

4.3. Clinical Significance for Joint Protection and Fall Prevention

From a clinical perspective, the observed reduction in knee flexion ROM has significant implications for joint protection, particularly regarding the patellofemoral joint. In a conventional low-seated STS, the knee flexion angle increases the contact stress between the patella and the femoral trochlea [21,22], which can be a primary source of pain for older adults with patellofemoral osteoarthritis or anterior knee pain. On the other hand, by optimizing the ascent path, the BSTS device provides a mechanical advantage that reduces the tensile load on the quadriceps during the critical

 doi:10.20944/preprints202604.0744.v1

initiation phase. By reducing peak knee joint angles, the biomimetic trajectory effectively minimizes the patellofemoral compressive forces that are typically exacerbated during deep-seated transitions.

Furthermore, the high effect sizes across all functional groups suggest a standardization of movement. While conventional chairs allow for high inter-individual variability in rising strategies—often leading to erratic and unsafe patterns in frail users. The BSTS effectively homogenizes the kinematics. By providing a guided, repeatable path, the device ensures that even low-functioning individuals can achieve the kinematic efficiency typically reserved for their high-functioning counterparts, thereby reducing the cognitive and physical effort required for daily mobility.

4.4. Limitations

Despite the significant biomechanical insights gained, several limitations should be acknowledged. First, the use of MediaPipe-based 2D pose estimation, while highly accessible and non-invasive, is inherently limited to sagittal-plane analysis. This approach may not fully capture three-dimensional trunk rotations or mediolateral instability, which are critical factors in fall risk assessment for frail older adults. Future studies should consider multi-camera setups to validate these kinematic findings in 3D space.

Second, the sample size of 30 participants (approximately 10 per functional group) is relatively modest. While the large effect sizes (η^2_p >.70 for kinematics; η^2_p =.42 for kinetics) suggest that the study was sufficiently powered to detect the primary effects of the seating condition, the non-significant interaction effects observed for I_{arm} (p=.21) might have been influenced by the limited sample size. Future studies with a larger cohort are needed to further validate the differential assistance patterns across diverse functional levels. Finally, this study focused on immediate biomechanical effects in a simulated environment. Longitudinal research is required to determine whether the long-term use of such biomimetic assistive devices leads to muscle disuse atrophy or, conversely, improves functional independence by reducing daily fatigue and pain.

5. Conclusions

This study successfully quantified the biomechanical efficacy of the BSTS through a synchronized AI-kinematic and kinetic assessment framework. Our results demonstrate that the device's unique forward-and-upward trajectory facilitates an early anterior displacement of the COM, significantly reducing the required ROM at the hip and knee joints while minimizing the need for compensatory trunk flexion. Furthermore, the integration of instrumented armrests revealed that the device substantially unloads the upper extremities, particularly during the critical momentum-transfer phase. These findings provide a strong evidence-based foundation for the use of trajectory-informed assistive technology to enhance toileting safety and preserve functional dignity in the aging population. By bridging the gap between automated pose estimation and kinetic sensing, this research offers a scalable model for evaluating assistive devices in ecologically valid settings.

Author Contributions: Conceptualization, S.-J.,Yeh, and Y.-S.,Yang; methodology, S.-Y.,Yang and Y.-S.,Yang; software, L.-C.,Chao and Y.-S.,Yang; validation, S.-J.,Yeh, S.-Y.,Yang, and T.-S.,Lu; formal analysis, S.-J.,Yeh, and Y.-S.,Yang; investigation, S.-J.,Yeh, S.-Y.,Yang, and T.-S.,Lu.; resources, L.-C.,Chao; data curation, S.-J.,Yeh, and S.-Y.,Yang; writing—original draft preparation, S.-J.,Yeh; writing—review and editing, Y.-S.,Yang. All authors have read and agreed to the published version of the manuscript.

Funding: This research was funded by Kaohsiung Medical University Industry-Academia Research Grant, grant number ST113018.

Data Availability Statement: The data presented in this study are available on request from the corresponding author due to ethical and privacy considerations as mandated by the Institutional Review Board of Kaohsiung Medical University Chung-Ho Memorial Hospital.

 doi:10.20944/preprints202604.0744.v1

Acknowledgments: In this section, you can acknowledge any support given which is not covered by the author contribution or funding sections. This may include administrative and technical support, or donations in kind (e.g., materials used for experiments). Where GenAI has been used for purposes such as generating text, data, or graphics, or for study design, data collection, analysis, or interpretation of data, please add "During the preparation of this manuscript/study, the author(s) used [tool name, version information] for the purposes of [description of use]. The authors have reviewed and edited the output and take full responsibility for the content of this publication.".

Conflicts of Interest: The authors declare no conflicts of interest.

Abbreviations

The following abbreviations are used in this manuscript:

STS	Sit-to-Stand
COM	Center-of-Mass
ROM	Range of Motion
BSTS	Biomimetic Stand-assist Toilet Seat
CST	Chair Stand Test
RGB	Red-Green-Blue

References

1. Janssen, W. G.; Bussmann, H. B.; Stam, H. J. Determinants of the sit-to-stand movement: a review. *Phys. Ther.* **2002**, *82* (9), 866-879.
2. Kotake, T.; Dohi, N.; Kajiwara, T.; Sumi, N.; Koyama, Y.; Miura, T. An analysis of sit-to-stand movements. *Arch. Phys. Med. Rehabil.* **1993**, *74* (10), 1095-1099.
3. Reisman, D. S.; Scholz, J. P.; Schöner, G. Coordination underlying the control of whole body momentum during sit-to-stand. *Gait & posture* **2002**, *15* (1), 45-55.
4. Guralnik, J. M.; Simonsick, E. M.; Ferrucci, L.; Glynn, R. J.; Berkman, L. F.; Blazer, D. G.; Scherr, P.; Wallace, R. B. A short physical performance battery assessing lower extremity function: association with. *J. Gerontol.* **1994**, *49* (2), M85-M94.
5. Thapa, P. B.; Gideon, P.; Fought, R. L.; Kormicki, M.; Ray, W. A. Comparison of clinical and biomechanical measures of balance and mobility in elderly nursing home residents. *J. Am. Geriatr. Soc.* **1994**, *42* (5), 493-500.
6. Lipsitz, L. A.; Jonsson, P. V.; Kelley, M. M.; Koestner, J. S. Causes and correlates of recurrent falls in ambulatory frail elderly. *J. Gerontol* **1991**, *46* (4), M114-M122.
7. Nevitt, M. C.; Cummings, S. R.; Kidd, S.; Black, D. Risk factors for recurrent nonsyncopal falls: a prospective study. *JAMA* **1989**, *261* (18), 2663-2668.
8. Hetherington-Rauth, M.; Magalhães, J. P.; Alcazar, J.; Rosa, G. B.; Correia, I. R.; Ara, I.; Sardinha, L. B. Relative sit-to-stand muscle power predicts an older adult's physical independence at age of 90 yrs beyond that of relative handgrip strength, physical activity, and sedentary time: a cross-sectional analysis. *Am. J. Phys. Med. Rehabil.* **2022**, *101* (11), 995-1000.
9. Marques, E. A.; Baptista, F.; Santos, D. A.; Silva, A. M.; Mota, J.; Sardinha, L. B. Risk for losing physical independence in older adults: the role of sedentary time, light, and moderate to vigorous physical activity. *Maturitas* **2014**, *79* (1), 91-95.
10. Schenkman, M.; Berger, R. A.; Riley, P. O.; Mann, R. W.; Hodge, W. A. Whole-body movements during rising to standing from sitting. *Phys. Ther.* **1990**, *70* (10), 638-648.
11. Papa, E.; Cappozzo, A. Sit-to-stand motor strategies investigated in able-bodied young and elderly subjects. *J. Biomech.* **2000**, *33* (9), 1113-1122.
12. Sadeh, S.; Gobert, D.; Shen, K.-H.; Foroughi, F.; Hsiao, H.-Y. Biomechanical and neuromuscular control characteristics of sit-to-stand transfer in young and older adults: a systematic review with implications for balance regulation mechanisms. *Clin. Biomech.* **2023**, *109*, 106068.

 doi:10.20944/preprints202604.0744.v1

13. Kim, J.-W.; Choi, J.-Y.; Ha, E.-J.; Choi, J.-H. Human pose estimation using mediapipe pose and optimization method based on a humanoid model. *Appl. Sci.* **2023**, *13* (4), 2700.
14. Singh, A. K.; Kumbhare, V. A.; Arthi, K. Real-time human pose detection and recognition using mediapipe. In *International conference on soft computing and signal processing*, 2021; Springer: pp 145-154.
15. Alexander, N. B.; Koester, D. J.; Grunawalt, J. A. Chair design affects how older adults rise from a chair. *J. Am. Geriatr. Soc.* **1996**, *44* (4), 356-362.
16. Bateni, H.; Maki, B. E. Assistive devices for balance and mobility: benefits, demands, and adverse consequences. *Arch. Phys. Med. Rehabil.* **2005**, *86* (1), 134-145.
17. Hughes, M.; Weiner, D.; Schenkman, M.; Long, R.; Studenski, S. Chair rise strategies in the elderly. *Clin. Biomech.* **1994**, *9* (3), 187-192.
18. Pai, Y.-C.; Naughton, B.; Chang, R. W.; Rogers, M. Control of body centre of mass momentum during sit-to-stand among young and elderly adults. *Gait & Posture* **1994**, *2* (2), 109-116.
19. Baer, G. D.; Ashburn, A. M. Trunk movements in older subjects during sit-to-stand. *Arch. Phys. Med. Rehabil.* **1995**, *76* (9), 844-849.
20. Van Lummel, R. C.; Evers, J.; Niessen, M.; Beek, P. J.; Van Dieën, J. H. Older adults with weaker muscle strength stand up from a sitting position with more dynamic trunk use. *Sensors* **2018**, *18* (4), 1235.
21. Hungerford, D. S.; Barry, M. Biomechanics of the patellofemoral joint. *Clin. Orthop. Relat. Res.* **1979**, *144*, 9-15.
22. Huberti, H. H.; Hayes, W. C. Patellofemoral contact pressures. The influence of q-angle and tendofemoral contact. *JBJS* **1984**, *66* (5), 715-724.